



In situ TPO/Raman to characterize single-walled carbon nanotubes

Jose E. Herrera, Daniel E. Resasco *

*School of Chemical Engineering and Materials Science, University of Oklahoma, 100 East Boyd St., Room T335,
Norman, OK 73019, USA*

Received 4 April 2003; in final form 12 May 2003

Published online: 2 July 2003

Abstract

Temperature programmed oxidation (TPO) coupled with in situ Raman spectroscopy has been used as an effective qualitative and quantitative analysis of raw and purified single-walled carbon nanotubes (SWNT) samples. The incorporation of Raman facilitates the identification of the nature of the oxidation peaks present in a TPO profile. Using different samples it was possible to evaluate the potential of the technique for quantifying different impurities in the SWNT samples as well as in SWNT-polymer composites.

© 2003 Elsevier B.V. All rights reserved.

1. Introduction

Since their discovery, single-walled carbon nanotubes (SWNT) have stimulated worldwide interest due to their fascinating physical and chemical properties that have opened a vast number of potential applications [1,2]. The methods developed for producing SWNT are diverse. These methods range from electric arc discharge and laser ablation of carbon targets containing metals to direct decomposition of carbon-containing molecules over metal catalysts [3–6]. Among the different alternatives explored in the last few years for production of SWNT, the catalytic decomposition of carbon-containing mole-

cules appears as a promising technique since it has the potential to be scaled-up at a relatively low cost, enabling applications that require large SWNT quantities [7].

In addition to SWNT, the raw material obtained by any of the methods mentioned above contains varying degrees of carbon impurities such as amorphous carbon, graphite fibers as well as residual metals from the catalyst used in the production [8–12]. Hence, a crucial step on the production of SWNT is a reliable characterization of the type and amounts of impurities present on a given sample. Electron microscopy (TEM/SEM) and thermal gravimetric analysis (TGA) have been used to obtain mostly qualitative assessments of the various carbon species present on a given sample and a quantitative measurement of the overall concentration of residual metals, respectively [13–16].

* Corresponding author. Fax: 1-405-325-5813.

E-mail address: resasco@ou.edu (D.E. Resasco).

We have previously proposed the temperature programmed oxidation (TPO) method as a useful tool for quantifying the amount of SWNT present on a sample [17] since when embedded in the catalyst SWNT burn in narrow temperature range, below the temperature in which MWNT, graphite, and carbon fibers are oxidized, but above the temperature at which amorphous carbon species are oxidized [18].

At the same time, Raman spectroscopy is an exceptionally powerful technique for characterizing the structure of SWNT. The Raman-allowed phonon mode E_{2g} , has extensively been used as a measure of the presence of ordered carbon, while the so-called D band is related to defects or the presence of nanoparticles and amorphous carbon [19,20]. Hence, the size of the D band relative to the G band can be used as a qualitative measurement for the formation of undesired forms of carbon. Nevertheless an accurate quantitative account of the different types of carbonaceous materials present on the sample cannot be obtained by Raman spectroscopy.

In this contribution, we present the results of a novel combination of these two techniques. By using a specifically designed cell, we have conducted in situ Raman spectroscopy during TPO. This particular combination of techniques has allowed us to identify the different carbonaceous species present in raw and purified SWNT samples, as well as to investigate the effect of residual metal catalysts in the SWNT reactivity. Additionally, to further explore the potential of this technique a composite prepared using SWNT and a polymer has been investigated.

2. Experimental

2.1. Materials and treatments

Several nanotube samples were analyzed. One of them was a raw sample as obtained from CNI produced by the HiPCO process, which as it is well known its major impurity is residual Fe catalyst [11]. This sample was also investigated after a purification step in nitric acid used to remove the residual iron species present. A couple of samples

prepared by catalytic disproportionation of CO over solid catalysts were also investigated. One of them was obtained over an unselective Co–W catalyst and the other over a highly selective Co–Mo catalyst. The synthesis of SWNT with varying selectivities by using this method has been previously reported [21,22]. In brief, the selective SWNT sample was obtained using a bimetallic Co–Mo catalyst with a total metallic loading of 2 wt% and a Co:Mo molar ratio of 1:3. Prior to the production of SWNT by CO disproportionation, the catalyst was heated in H_2 flow to 500 °C, and then heated in He flow to 850 °C. To effect the SWNT growth, CO was fed to the reactor for 2 h at a total pressure of 5 atm.

A SWNT-filled polystyrene composite was also analyzed. This particular material contains 2 wt% of SWNT dispersed on the polymer matrix and was prepared by miniemulsion polymerization. The details of its preparation have been reported elsewhere [23].

2.2. Temperature programmed oxidation analysis

To conduct the TPO analysis, a continuous flow (50 cm^3/min) of 2% O_2 in He was passed over the sample while the temperature was linearly increased at a rate of 12 °C/min. To enhance the sensitivity of the technique, the CO_2 and CO produced during the oxidation are quantitatively converted to methane in a methanator [24], where the stream coming from the TPO is passed with a 50 cm^3/min stream of H_2 over a 15% Ni/ γ - Al_2O_3 catalyst at 400 °C. The evolution of the methane produced in the methanator quantitatively corresponds to the CO_2 and CO generated in the TPO is monitored in a flame ionization detector, SRI Model 110 FID. Quantification of the evolved CO and CO_2 , calibrated with 100 μl pulses of pure CO_2 and oxidation of known amounts of graphite gives a direct measurement of the amount of carbon that gets oxidized at each temperature.

2.3. In situ Raman spectroscopy

The Raman spectra were obtained in a Jovin Yvon-Horiba Lab Raman equipped with a CCD detector and with three different laser excitation

sources, having wavelengths of 633 (He–Ne laser), 514 and 488 nm (Ar laser). This system is equipped with an in situ reaction chamber that can be heated up to more than 1000 °C under flowing gases. Before each spectrum was acquired, the sample was placed in the in situ cell and then exposed to a continuous flow of a mixture of 2% O₂ in He while the temperature was linearly increased at a rate of 12 °C/min, reproducing the exact conditions of the TPO. The heating was stopped at a given temperature and, to obtain the Raman spectrum, the sample was cooled down to room temperature under the same flow. To make meaningful comparisons, it is essential to acquire the spectra on the same spot of the sample every time this heating–cooling sequence is followed.

3. Results and discussion

Fig. 1 illustrates the TPO profiles of the carbonaceous species present on the raw and purified HiPCO materials. It was found that the amount of carbon present on both samples was 83% and 99%, respectively, as obtained from the quantification of the amount of CO and CO₂ evolved during the TPO process. This undoubtedly shows that most of the Fe present in the sample was removed by the purification process. However, a first comparison between both profiles would indicate that after purification there are three different carbonaceous species present on the purified material, each one showing a different behavior towards O₂ oxidation. Two of these new carbonaceous species (peak position 600 and 765 °C in the TPO profile shown in Fig. 1b) have been originated during the purification process. On the other hand, the first peak in the profile of the purified material (peak at 460 °C in Fig. 1a) is as the same position as the only peak observed for the raw SWNT.

To determine the kind of carbonaceous species present on the purified sample that are responsible for each one of the peaks appearing in the TPO profile, Raman spectroscopy was carried out on the raw and purified materials. For the purified material, Raman spectra were also acquired after each in situ oxidation step, that corresponds to the valleys in the TPO profiles, i.e., the spectra were

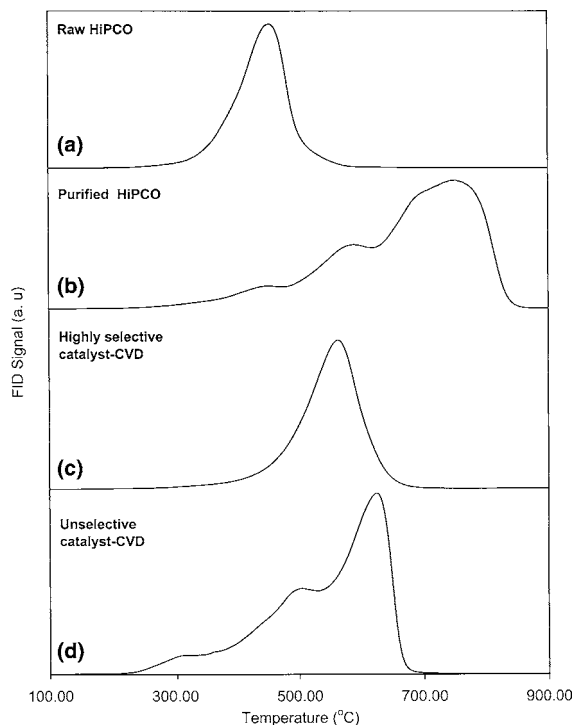


Fig. 1. Temperature programmed oxidation (TPO) profiles of the carbonaceous species present in (a) raw HiPCO material, (b) purified HiPCO material, (c) the product obtained by CVD over a highly selective Co–Mo catalyst and (d) the product obtained by CVD over an unselective Co–W catalyst. The profiles were obtained using a mixture of 5% of O₂ in He at a heating rate of 12 °C/min.

acquired at room temperature and then after a oxidation steps at 400, 500 and 630 °C under the same conditions used to get the TPO profiles, to determine the changes in the Raman spectra after elimination of the corresponding species.

Figs. 2 and 3 summarize the results of this study. Relatively small variations are observed between the Raman spectra of the raw and purified samples, or even among the spectra of the purified sample after each consecutive oxidation step, indicating that SWNT are undoubtedly the main carbon species present on both purified and raw samples. However, clear trends are still possible to observe. First, a decrease in the intensity of the D band is observed when comparing the raw HiPCO material with the purified sample, indicating that the purification procedure not just removes the

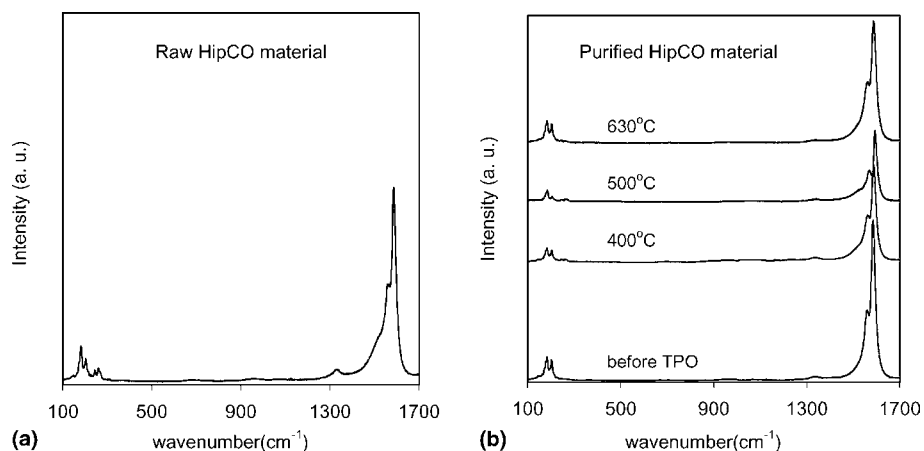


Fig. 2. Resonant Raman spectra obtained for (a) raw HiPCO material at room temperature and (b) purified HiPCO material before and after subsequent in situ oxidation steps at 400, 500 and 630 °C. The laser excitation wavelength was 514 nm.

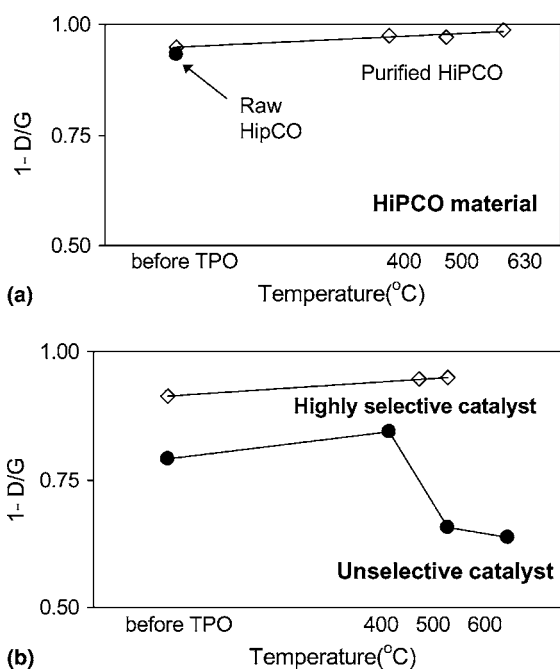


Fig. 3. Contributions of the D band to the Raman spectra for: (a) the HiPCO purified materials before and after subsequent in situ oxidation steps at 400, 500 and 630 °C (the data for the raw HiPCO sample is also shown for reference) and (b) two different carbon deposits obtained by CVD over a highly selective Co–Mo and over an unselective Co–W catalyst before and after subsequent in situ oxidation treatments at the indicated temperatures. The contributions of the D band to the Raman spectra is expressed using a quality parameter: $1 - D/G$; where D and G are the integrated areas of the D and G Raman bands, respectively.

residual Fe from the sample but also decreases the amount of amorphous carbon that might have been originated during the synthesis process. Second, as the oxidation temperature of the purified sample was increased, the relative contribution of the D band clearly decreased. This trend is better illustrated in Fig. 3a, which shows the gradual decrease of the D band in terms of the expression $(1 - D/G)$. This term may be considered a ‘quality parameter’ of the SWNT sample, since it qualitatively measures the amount of SWNT compared to other disordered carbon species. As we have reported before [17], amorphous and chemically impure carbon species are oxidized at temperatures below 400 °C, consequently subsequent oxidation steps remove increasing amounts of amorphous carbon material from the samples which results in the decrease of the relative intensity of the D band in the Raman spectra.

Although during these oxidation treatments disordered carbon was preferentially eliminated, based on the results obtained by Raman spectroscopy it is clear that the three peaks observed in the purified HiPCO sample do not correspond to different carbon species. As we have mentioned before, TPO is a catalytic process in which residual metal can have a significant impact. On the unpurified raw material, the amount of Fe is so high that all the different forms of carbon in the sample are essentially oxidized simultaneously at 460 °C.

By contrast, on the purified sample, the amount of iron present is considerably lower (just about 1%). Therefore, the catalytic influence of iron during the TPO process is smaller. Consequently, we attribute the difference between the TPO profiles of the raw and purified materials to the different amounts of iron present on these two materials. Accordingly, it is possible that both, the peak at 460 °C present in the TPO profile of the purified material and the single peak shown in the TPO of the raw SWNT sample are originated by SWNT contaminated with iron species. On the other hand, the peaks appearing at 500 and 630 °C in the purified sample are originated from SWNT associated to small or negligible amounts of metal.

A similar analysis was performed on two different raw SWNT materials synthesized by CO disproportionation on solid catalysts. One of them was obtained over a selective Co–Mo bimetallic catalyst, in which SWNT is the dominant product. The other sample was obtained over an unselective Co–W metallic catalyst, in which SWNT, MWNT, graphite and amorphous carbon are all present [17,22]. Figs. 1c and d show the TPO profiles of each of these two materials, respectively. It can be seen that the sample obtained over the selective catalyst, which contains mostly SWNT, displays a single TPO peak centered at 570 °C. However, an interesting difference is observed in this case compared to the TPO profile obtained for the raw HiPCO material shown in Fig. 1a. That is, although both profiles show a single main peak, the peak position for the SWNT obtained from the Co–Mo catalyst is at more than 100 °C higher than that for the HiPCO material. This difference is primarily due to the different amount of residual metal catalyst left in each sample. While the raw material obtained by the HiPCO process contains up to 30% in weight of iron [9,25], the sample obtained over the Co–Mo catalyst contains less than 2% of Co and Mo metal impurities [7]. Consequently, the material obtained by the HiPCO process has a larger amount of metallic species able to catalyze the oxidation reaction during the TPO process, lowering the temperature needed to oxidize the SWNT. In addition to the difference in the amount of residual metal in the two samples, another important difference is the presence of the

silica support on the raw material prepared from the Co–Mo/SiO₂ catalyst. The silica support is essentially a thermal insulator that may separate the SWNT bundles and consequently prevent the propagation of the oxidation.

To further characterize the material obtained over the selective Co–Mo catalyst, we used the in situ TPO/Raman technique. In this case, the in situ oxidation steps were performed at 450 and 500 °C under the same conditions used to get the TPO profiles. Fig. 4a shows the results that undoubtedly corroborate that the sample is mostly composed by SWNT. As in the case of the HiPCO material, there were some variations in the Raman spectra after the different TPO stages. A decrease in the contribution of the D band was observed after the higher oxidation temperatures. As with the HiPCO purified material, we integrated the areas of the G and D bands and calculated its relative area. Fig. 3b shows the results of the ‘quality parameter’ (1 – D/G), which is high even for the raw material, but clearly increases after the oxidation treatments. As mentioned above, below 450 °C amorphous and chemically impure carbon species are burned; therefore the first oxidation step eliminates the amorphous carbon material from the samples. This oxidation results in the decrease of the relative intensity of the D band in the Raman spectra. However, as shown in Figs. 3b and 4a, a subsequent oxidation step (500 °C) does not change the contribution of the D band to the spectra, since at this temperature all amorphous carbon has been removed.

A contrasting behavior is observed in the TPO profile of the material obtained over the unselective catalyst (see Fig. 1d). Instead of the single peak observed in the previous case, three oxidation peaks are obtained on this sample. To identify the nature of the species responsible for these peaks, in situ Raman spectroscopy was carried out on this sample. As before, the spectra were obtained at room temperature after each subsequent in situ oxidation steps at 400, 500 and 600 °C, under the same conditions used in the TPO experiments. Fig. 4b shows the Raman spectrum obtained in each case. It can be observed that the relative intensity of the D band is much stronger for this sample than for any of the other samples investi-

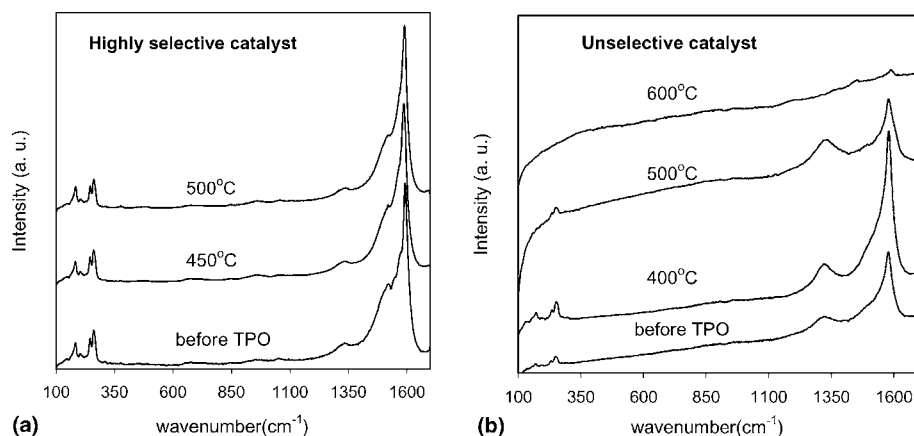


Fig. 4. Resonant Raman spectra for (a) the carbon deposits obtained over a highly selective Co–Mo catalyst. The spectra were acquired before and after subsequent in situ oxidation steps at 450 and 500 °C and for (b) the carbon deposits obtained over an unselective Co–W catalyst. The spectra were acquired before and after subsequent in situ oxidation steps at 400, 500 and 600 °C. The laser excitation wavelength was 514 nm.

gated. This clearly reveals the low selectivity of the particular catalyst used in this sample. In addition, there are other interesting changes in the Raman spectra that deserve further consideration. First, the relative area of the D band in each spectra changes after each subsequent oxidation step. This behavior is illustrated in Fig. 3b, which shows for the unselective catalyst a clear decrease on the D band contribution after the first oxidation step (400 °C). As previously stated, below this temperature amorphous carbon species are oxidized and, therefore this first oxidation step should eliminate most of the amorphous carbon present in the material, consequently, a decrease in intensity of the D band in the Raman spectrum is observed. A different behavior is observed after the oxidation step at 500 °C. In this case, an enhancement in the contribution of the D band to the overall spectra is observed. Evidently this behavior cannot be attributed to the presence of amorphous carbon in the sample, since all amorphous carbon species have been removed below this temperature. The enhancement in the D band should therefore be ascribed to a decrease in the amount of ordered forms of carbons in the sample. As mentioned above, SWNT are oxidized at a temperature below the oxidation threshold of MWNT and graphite [17]. In fact, the intensity of the D band in the Raman spectra suggests that

even after oxidation at 400 °C the sample is composed of SWNT and other forms of disordered carbon. All these together points to a decrease on the amount of SWNT and an increase on the relative amount of MWNT and (or) graphite in the sample after the 500 °C oxidation step, which in turn would be responsible for the increase of the intensity of the D band [26]. Finally, after the oxidation at 600 °C, most of the carbonaceous species have been oxidized as shown by the TPO profile. Moreover, the low intensity of the bands in the Raman spectrum is consistent with a small amount of refractory graphite still present in the sample.

To further evaluate the potential of this technique to characterize SWNT-based polymer composites, a composite containing 2 wt% SWNT dispersed in a polystyrene matrix was analyzed. The spectroscopic and chemical analysis of this kind of materials is rather challenging due to the small amount of SWNT in the sample. Fig. 5a shows the TPO profile of the composite. Under these conditions, a single peak centered at 450 °C is observed. Previous TGA studies indicate that the burning temperature of polystyrene in pure air is around 400 °C [23], so we assign the peak at 450 °C to the oxidation of polystyrene. The oxidation of SWNT does not show a separate TPO peak. It is most likely that this peak is masked inside the

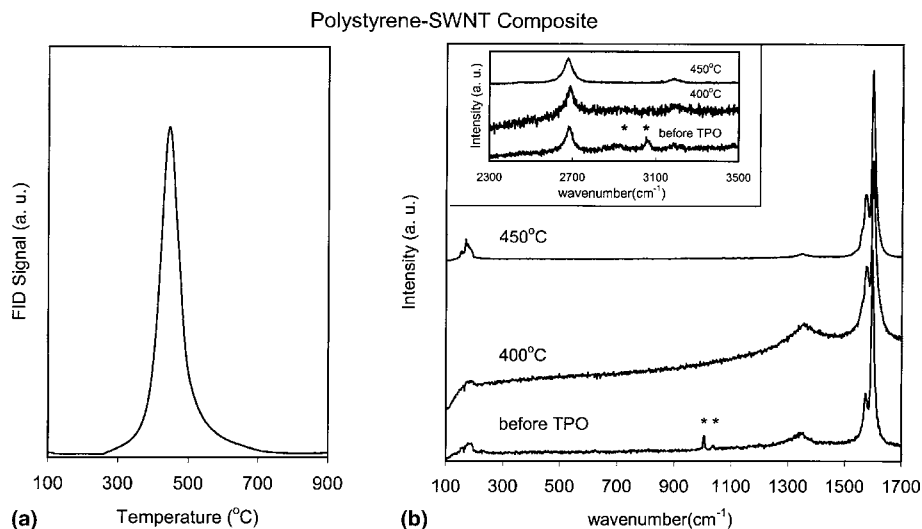


Fig. 5. (a) Temperature programmed oxidation (TPO) profile of the carbonaceous species present in a polystyrene-SWNT composite. The profile was obtained using a mixture of 5% of O_2 in He at a heating rate of $12\text{ }^\circ\text{C}/\text{min}$. (b) Resonant Raman spectra obtained for polystyrene-SWNT. The spectra were acquired before and after subsequent in situ oxidation steps at 400 and $450\text{ }^\circ\text{C}$. The (*) symbol indicates Raman bands of polystyrene. The laser excitation wavelength was 514 nm .

main peak, which goes up to $700\text{ }^\circ\text{C}$. Therefore, to help characterizing the oxidation of SWNT inside the polymer, we employed the in situ TPO/Raman technique. In this case, the in situ oxidation steps were performed at 400 and $450\text{ }^\circ\text{C}$ under the same conditions used to get the TPO profiles.

Fig. 5b shows the Raman spectra of the composite before any in situ TPO treatment. From this result a major contribution of SWNT to the overall spectrum is apparent. In contrast to the TPO profile that showed a single peak mainly due to the oxidation of the polymer; the bands corresponding to SWNT dominate the Raman spectrum of the material. The reason for this apparent contrasting behavior on the Raman spectrum is the extremely high quantum efficiency of Raman scattering for SWNT throughout a resonant process, while very low Raman signals are obtained for the polymer film. Nevertheless, some bands arising from the polymer can be clearly observed. For example in the low frequency region the peaks between 1000 and 1060 cm^{-1} must be attributed to ring vibration or in plane C–H deformation of the polystyrene moiety [27]. In the high frequency region some other polymer bands are also present.

Two distinct peaks of appreciably large intensities around 2915 and 3058 cm^{-1} are apparent. The former band originates from C–H chain vibration (C–H stretch mode) in the polystyrene. The latter peak is related to C–H radial stretch in the benzene rings of the polymer. We must note that the bands at 2700 and 3200 cm^{-1} are second-order Raman bands of SWNT and are not originated from the polystyrene.

After the first oxidation step at $400\text{ }^\circ\text{C}$ there is a dramatic change in the Raman spectrum of the composite. It is clear that the relative intensity of the bands of the polymer respect to the ones for SWNT has significantly decreased. In fact, the polymer bands between 1000 and 1060 cm^{-1} have disappeared in the background of the spectrum, while the bands at 2915 and 3058 cm^{-1} are barely observed. After a second oxidation stage at $450\text{ }^\circ\text{C}$, all the bands from the polystyrene disappear and the Raman spectrum only shows the typical bands of bare SWNT. However, it cannot be completely ruled out that some polystyrene may still remain in the sample, as the signal of the SWNT is orders of magnitude higher than that of the polymer.

4. Conclusions

A novel in situ Raman spectroscopic analysis coupled with TPO has shown to be a powerful tool to conduct systematic qualitative and quantitative characterization of raw and purified SWNT materials. The presence of contamination in the form of metallic species has shown to deeply affect the TPO profiles. However, in situ Raman spectroscopy has allowed us to clearly identify the nature of the peaks and describe the oxidation processes responsible for each TPO peak. A polymer-SWNT composite has also been analyzed by this technique. In this case, the resonant Raman effect on SWNT and the low scattering efficiencies of polymer films complicate the quantitative analysis of the data.

Acknowledgements

This research was conducted with financial support from the Department of Energy, Office of Basic Energy Sciences (Grant No. DE-FG03-02ER15345). J.E.H. thanks the Fulbright-CAREC program for a scholarship.

References

- [1] S. Iijima, T. Ichihashi, *Nature* 363 (1993) 603.
- [2] B.I. Yakobson, R.E. Smalley, *Am. Sci.* 85 (1997) 324.
- [3] P. Nikolaev, M.J. Bronikowski, R.K. Bradley, F. Rohmund, D.T. Colbert, K.A. Smith, R.E. Smalley, *Chem. Phys. Lett.* 313 (1999) 91.
- [4] J.A. Kong, A.M. Cassell, H. Dai, *Chem. Phys. Lett.* 292 (1998) 567.
- [5] R.K. Rana, Y. Koltypin, A. Gedanken, *Chem. Phys. Lett.* 344 (2001) 256.
- [6] R. Sen, A. Govindaraj, C.N.R. Rao, *Chem. Mater.* 9 (1997) 2078.
- [7] D.E. Resasco, W.E. Alvarez, F. Pompeo, L. Balzano, J.E. Herrera, B. Kitiyanan, A. Borgna, *J. Nanoparticle Res.* 4 (2002) 131.
- [8] A. Peigney, P. Coquay, E. Flahaut, R.E. Vandenberghe, E. De Grave, C. Laurent, *J. Phys. Chem. B* 105 (2001) 9699.
- [9] A.S. Lobach, N.G. Spitsina, S.V. Terekhov, E.D. Obraztsova, *Phys. Solid State* 44 (2002) 475.
- [10] B. Zhao, H. Hu, S. Niyogi, M.E. Itkis, M.A. Hamon, P. Bhowmik, M.S. Meier, R.C. Haddon, *J. Am. Chem. Soc.* 123 (2001) 11673.
- [11] I.W. Chiang, B.E. Brinson, A.Y. Huang, P.A. Willis, M.J. Bronikowski, J.L. Margrave, R.E. Smalley, R.H. Hauge, *J. Phys. Chem. B* 105 (2001) 8297.
- [12] C.M. Yang, K. Kaneko, M. Yudasaka, S. Iijima, *NanoLett.* 2 (2002) 385.
- [13] C.N.R. Rao, B.C. Satishkumar, A. Govindaraj, M. Nath, *Chem. Phys. Chem.* 2 (2001) 78.
- [14] A.G. Rinzler, J. Liu, H. Dai, P. Nikolaev, C.B. Huffman, F.J. Rodriguez-Macias, P.J. Boul, A.H. Lu, D. Heymann, D.T. Colbert, R.S. Lee, J.E. Fischer, A.M. Rao, P.C. Eklund, R.E. Smalley, *Appl. Phys. A* 67 (1998) 29.
- [15] Z. Shi, Y. Lian, F. Liao, X. Zhou, Z. Gu, Y. Zhang, S. Iijima, *Solid State Commun.* 112 (1999) 35.
- [16] D.E. Resasco, J.E. Herrera, in: H.S. Nalwa (Ed.), *Encyclopedia of Nanoscience and Nanotechnology*, American Scientific Publishers, 2003, in press.
- [17] B. Kitiyanan, W.E. Alvarez, J.H. Harwell, D.E. Resasco, *Chem. Phys. Lett.* 317 (2000) 497.
- [18] W.E. Alvarez, B. Kitiyanan, A. Borgna, D.E. Resasco, *Carbon* 39 (2001) 547.
- [19] R. Saito, M. Fujita, G. Dresselhaus, M.S. Dresselhaus, *Appl. Phys. Lett.* 60 (1992) 2204.
- [20] W.E. Alvarez, F. Pompeo, J.E. Herrera, L. Balzano, D.E. Resasco, *Chem. Mater.* 14 (2002) 1853.
- [21] J.E. Herrera, L. Balzano, A. Borgna, W.E. Alvarez, D.E. Resasco, *J. Catal.* 204 (2001) 129.
- [22] J.E. Herrera, D.E. Resasco, *J. Phys. Chem.* 107 (2003) 3738.
- [23] H.J. Barraza, F. Pompeo, E.A. O'Rear, D.E. Resasco, *NanoLett.* 2 (2002) 797.
- [24] S.C. Fung, C.A. Querini, *J. Catal.* 138 (1992) 240.
- [25] M. Yudasaka, H. Kataura, T. Ichihashi, L.C. Qin, S. Kar, S. Iijima, *NanoLett.* 1 (2001) 487.
- [26] J. Kastner, T. Pichler, H. Kuzmany, S. Curran, W. Blau, D.N. Weldon, M. Delamesiere, S. Draper, H. Zandbergen, *Chem. Phys. Lett.* 221 (1994) 53.
- [27] W.M. Sears, J.L. Hunt, J.R. Stevens, *J. Chem. Phys.* 75 (1981) 1589.